Quaternary Research (2017), **87**, 24–36.

doi:10.1017/qua.2016.5

Properties, age, and significance of dunes near Snow Water Lake, Elko County, Nevada

Jeffrey S. Munroe*, Andrew L. Gorin, Noah N. Stone, William H. Amidon
Geology Department, Middlebury College, Middlebury, VT 05753, United States

(Received June 7, 2016; Accepted October 12, 2016)

Abstract

Dunes adjacent to the Snow Water Lake playa in Elko County of northeastern Nevada rise up to ~10 m above the playa surface in seven distinct clusters. The dunes are composed of tan silty loam containing calcite, quartz, plagioclase, and dioctahedral clay. Abundances of trace elements, along with relative proportions of quartz and calcite, are distinct between dunes along the north and south sides of the playa, reflecting proximity to streams draining different lithologies in the neighboring mountains. Luminescence (optically stimulated luminescence and infrared-stimulated luminescence) dating of dune crest samples demonstrates that the last episode of dune accumulation occurred in the mid-eighteenth century. Moisture-sensitive tree ring records from a nearby site indicate that dune accumulation coincided with an interval of below-average precipitation immediately following a very wet decade. This sequence is consistent with models requiring wetter climatic conditions to move coarse sediment onto a playa surface, followed by dune building under drier conditions. Younger luminescence ages from a sand-dominated unit exposed in an arroyo cut through the dunes may reflect a wetter, more erosive climatic regime ca. AD 1800. The Snow Water Lake dunes are currently eroding, signaling a reduction in the amount of sediment reaching the playa.

Keywords: Dunes; Luminescence; Great Basin; Holocene; Tree rings

INTRODUCTION

Small clusters of dunes are common features on valley bottoms within the Great Basin of the southwestern United States. In contrast to the more extensive eolian systems of the western High Plains (e.g., Ahlbrandt and Fryberger, 1980; Muhs et al., 1996; Muhs and Wolfe, 1999; Muhs and Holliday, 2001), relatively little research has focused on these features. Nonetheless, there are a variety of reasons why these isolated dune clusters are significant. For instance, these dunes, which are commonly adjacent to playas on valley floors previously flooded by Pleistocene pluvial lakes, are important records of Holocene hydroclimatic variability. Because few of these dune complexes have been dated, the acquisition of additional age control is fundamental to efforts to identify regional patterns of eolian activity (Halfen et al., 2016). Furthermore, as local high points within relatively flat landscapes, and with a soil texture that strongly contrasts with their surroundings, these dunes represent crucial habitat diversity for flora and fauna (Lancaster and Mahan, 2012). For similar reasons, they may also have been significant for Native Americans (Grayson, 2011).

This study was undertaken to determine when dunes adjacent to the Snow Water Lake playa in northeastern Nevada were last actively accumulating. Here we describe the distribution of these dunes, discuss their physical properties, and explore the significance of their ages through comparison with local paleoclimate records and established models for climatic controls on dune activity.

SETTING

The dunes targeted in this study, hereafter referred to as the "Snow Water Lake dunes," are located in Elko County ~30 km south of Wells, Nevada (Fig. 1). The dunes are concentrated in seven clusters adjacent to the Snow Water Lake playa, which covers an area of ~16 km^2 at an elevation of 1706 meters above sea level (m asl) at the eastern foot of the East Humboldt Mountains (Fig. 1). The dunes stand up to about 10 m above the playa surface and are composed of tan silty loam. This loam is locally cemented by calcium carbonate (Fig. 2), but in general, the sediment is loose and unconsolidated. Elevations within individual clusters of dunes rise steeply on their western sides and taper gently to the east. The dunes have a compound morphology and appear stabilized with a "melted" appearance, rounded contours, and

*Corresponding author at: Geology Department, Middlebury College, Middlebury, VT 05753, United States. E-mail address: jmunroe@middlebury.edu (J.S. Munroe).

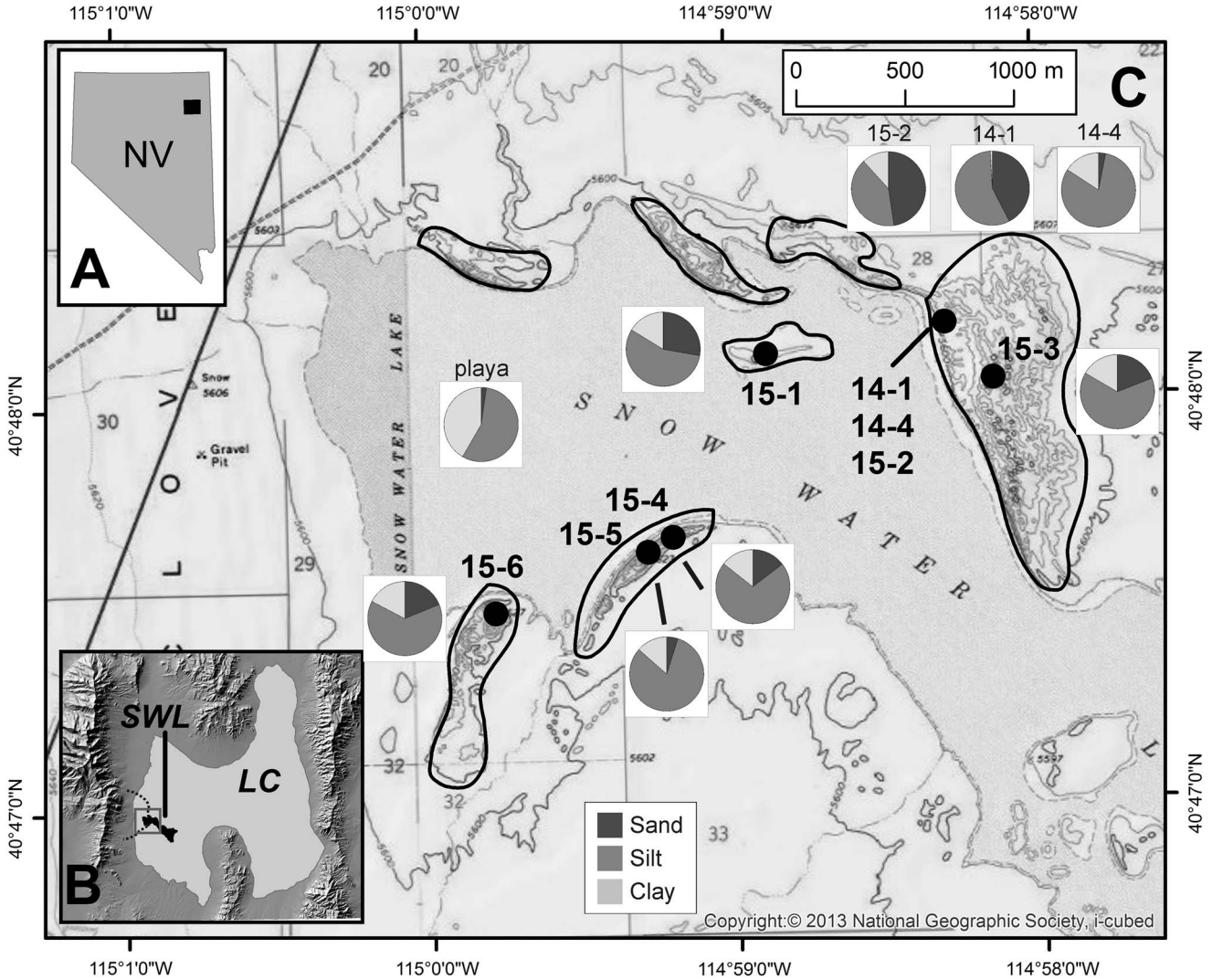

Figure 1. (A) Map showing the location of the study area in northeastern Nevada. (B) Location of the Snow Water Lake (SWL) playa (black) in the southwestern sector of the area formerly inundated by pluvial Lake Clover (LC, light gray). Gray box outlines the study area at the western end of the playa highlighted in panel C. Dotted lines highlight Wiseman Creek, draining the metamorphic core complex northwest of Snow Water Lake, and Warm Creek, draining carbonate terrane to the southwest. (C) US Geological Survey 7.5-minute base map (Snow Water Lake and Gordon Creek quadrangles) showing the study area at the western end of Snow Water Lake. Black lines delineate dune clusters. Locations of samples collected in 2014 and 2015 are shown, as are pie charts illustrating the abundance of sand/silt/clay (for clarity, grain-size data are not presented for all samples). The legend for these grain-size categories is shown at the bottom.

lack of active slip faces (Fig. 2). The dunes are sparsely vegetated with greasewood and appear to be eroding; shrubs perch atop root-bound pedestals of sediment, demonstrating recent surface lowering, and surface sediments are commonly coarser than underlying material, suggesting winnowing of fines.

The Snow Water Lake area has a continental climate with a mean annual temperature of 7.5°C and mean annual precipitation of 350 mm, measured at National Weather Service cooperative site 261740. Mean monthly temperatures peak in July (29.7°C) and August (29.1°C) and are lowest in December (3.6°C) and January (2.6°C). July and August are both very dry, averaging <16 mm of precipitation. January has the greatest average precipitation (45 mm), followed closely by November, December, and February (~38 mm). Spring months average ~30 mm of precipitation. Wind data are available for Elko, Nevada, ~70 km to the west where mean monthly wind speeds are highest in in the spring, reaching a maximum of 3.2 m/s in April. December has the lowest mean wind speed (2.2 m/s). Wind directions are dominantly from the west between March and October and from the east in the winter.

Several streams draining the East Humboldt Mountains extend eastward toward the Snow Water Lake playa. All of these are ephemeral or have been diverted for irrigation. Numerous springs are also present in the Snow Water Lake watershed (Bureau of Land Management [BLM], 2012), but none of them contribute water directly to the playa.

https://doi.org/10.1017/qua.2016.5

Figure 2. (color online) Field photographs of the Snow Water Lake dunes. (A) View across the flat playa surface toward the steep western face of the dunes near the site of sample 15-6. (B) View of the crest of the dune cluster near sample 15-3 showing the sparse vegetation, lack of slip faces, and overall "melted" appearance of the dunes. (C) Excavation at site 15-3 showing visible internal stratigraphy highlighted by bands of carbonate. (D) Close-up of the excavation at site 15-3 showing internal stratigraphy and the optically stimulated luminescence sample tube before it was removed.

As a result, the playa surface is dry except during the wettest years. Weakly developed shorelines, delineated by stranded driftwood and subtle evidence of wave erosion, are present at ~1 m and ~2 m above the playa along its north side (Fig. 3). These features likely correspond to high-water during the mid-1980s (BLM, 2012). Continuous beach ridges are also clear 1–3 km to the north and east of the playa margin. On 7.5-minute topographic maps, these features have crest elevations of ~1710 m asl, which is ~4 m above the playa, but still below the dune crests. The age of these ridges is unclear; however, they may represent final recessional stages of Lake Clover, a much larger (~900 km^2) pluvial lake that inundated the valley during the last glacial maximum (Fig. 1B). Radiocarbon dating of gastropod shells indicates that Lake Clover stood at its high-stand level of 1729 m asl ca. 19.5 cal ka BP and again ca. 17.0 cal ka BP (Munroe and Laabs, 2013). The timing of regression of Lake Clover is not known, although artifacts dating to the middle and late Archaic period have been reported from near Snow Water Lake, indicating that Lake Clover had disappeared by the middle Holocene (Nevada Archaeological Association, 2000).

METHODS

Field sampling

Despite a thorough reconnaissance, no deep natural exposures were located within the Snow Water Lake dunes. This reality, coupled with the objective of determining when the dunes were last accumulating, motivated a sampling strategy focused on hand excavations into dune crests. A few auxiliary samples were collected from other settings, but most samples and resulting age estimates pertain to the last period of active dune accumulation.

Field study in July 2014 focused on the dune clusters along the north side of the playa and on the larger concentration of dunes to the east (Fig. 1). Small reconnaissance excavations

https://doi.org/10.1017/qua.2016.5

Figure 3. (color online) Photograph of Snow Water Lake in July 1987 by Jeff Moore, Bureau of Land Management Office, Elko, Nevada (top). Subtle shorelines (highlighted by dashed lines) along the north side of the Snow Water Lake playa that may reflect high water during the 1980s (bottom).

were made in multiple locations, but sampling was confined to a single site in the eastern cluster where an arroyo wall was excavated by hand to access the dune stratigraphy (Fig. 4). Sediment was sampled for luminescence dating at the base of this exposure and in three locations within the uppermost meter of the dune (Fig. 4). Samples were also collected from the playa surface, from the arroyo bed, from the finer sediment comprising the central unit of the stratigraphy, and from the sun-dried crust at the surface (Table 1).

A second visit in July 2015 focused on expanding the spatial distribution of samples and cross-checking the results from 2014 (Table 1). One additional sample was taken from the coarse material near the base of the 2014 arroyo section, and five other dune crest samples were collected from the isolated dune "island" in the playa (15-1), the high point of the eastern dunes (15-3), and from the two dune clusters along the south side of the playa (Fig. 1). Excavations were made with a shovel, taking advantage of local steepenings in the topography.

Samples for luminescence dating were collected following standard protocols. After excavating an exposure (>70 cm below the dune surface), a 2.5-cm diameter metal tube was hammered in parallel to bedding or horizontally if bedding was indistinct (Fig. 2). The tube was excavated with a trowel and immediately capped, and surrounding material (~20 cm radius) was collected in a plastic bag for determination of the dose rate. A sealed sample was also taken for calculation of water content.

Analyses

In the laboratory, samples for grain-size analysis were deflocculated (minimum 3 days) in sodium hexametaphosphate, sonicated, and analyzed by laser scattering in a Horiba LA-950 particle sizer. This instrument reports grain-size distribution on a volume basis and has an effective range from 50 nm to 3 mm. A refractive index of 1.54 with an imaginary component of 0.1i was used for calculations. Duplicates were run on 10% of samples.

Geochemical assays were made by ALS Minerals on bulk samples. Samples were dried, homogenized, and split before submission, and they were analyzed with inductively coupled plasma mass spectrometry (ICP-MS) following powdering and lithium metaborate fusion.

Mineralogical composition of the dune samples was determined through X-ray diffraction (XRD) analysis on bulk samples. Samples were run as random powders and as oriented clay fractions in a Bruker D8 with CuKα radiation and a theta-theta goniometer. Samples were scanned from 2° to 70° 2θ at 3°/min. Slides were heated at 100°C for 1 h and run again to distinguish the 10Å peak of illite from halloysite. Analysis of XRD patterns using the software Eva permitted determination of the relative abundance of major minerals through measurement of peak areas. In this manner, quartz was represented by its 100 peak at 4.26 Å, potassium feldspar (002 at 3.24 Å), plagioclase (002 at 3.18 Å), and calcite (100 at 3.03 Å).

Luminescence samples were processed and analyzed in the Middlebury College Luminescence Lab under a 589-nm sodium lamp fitted with a Lee 101 filter screen. Following overnight treatments in 10% HCl and bleach, the 165–250-μm fraction underwent density separations with lithium heteropolytungstate to obtain quartz and potassium feldspar fractions. Quartz was etched in concentrated HF, and potassium feldspar was etched in 10% HF, both followed by an HCl rinse.

Sample analyses were performed on a Daybreak 2200 luminescence reader. Photons were recorded using a 9235QA photomultiplier tube manufactured by Electron Tubes with a dark count rate of roughly 20 cps. Stimulation was performed with blue LEDs (480 nm) for quartz and infrared LEDs (880 nm) for feldspar. Irradiations were performed using a 100 miC ^{90}Sr beta source manufactured by Eckert and Ziegler. Source calibration was performed with Riso batches 71 and 98.

All luminescence samples were analyzed using the single-aliquot regenerative-dose protocol for quartz (Murray and Wintle, 2000) and the postinfrared infrared protocol for K-feldspar (Buylaert et al., 2009). Quartz aliquots were ~6 mm in diameter (100s of grains), and feldspar aliquots were ~3 mm diameter (<100 grains). Both protocols involved six luminescence measurements: natural, regen-1, regen-2, regen-3, zero dose, and regen-1'. Data reduction was performed using the RLum package (version 4.1) to determine the equivalent dose, D_e (Kreutzer et al., 2012). Because shine down curves were slow (fast ratios of 5 to 10), we used an early background correction scheme that involved subtracting the measured counts in the first second from the measured counts in the fourth to fifth seconds. Estimates of D_e were screened using the recycling test, recuperation test, and the test-dose reproducibility ratio (the maximum difference between the

https://doi.org/10.1017/qua.2016.5

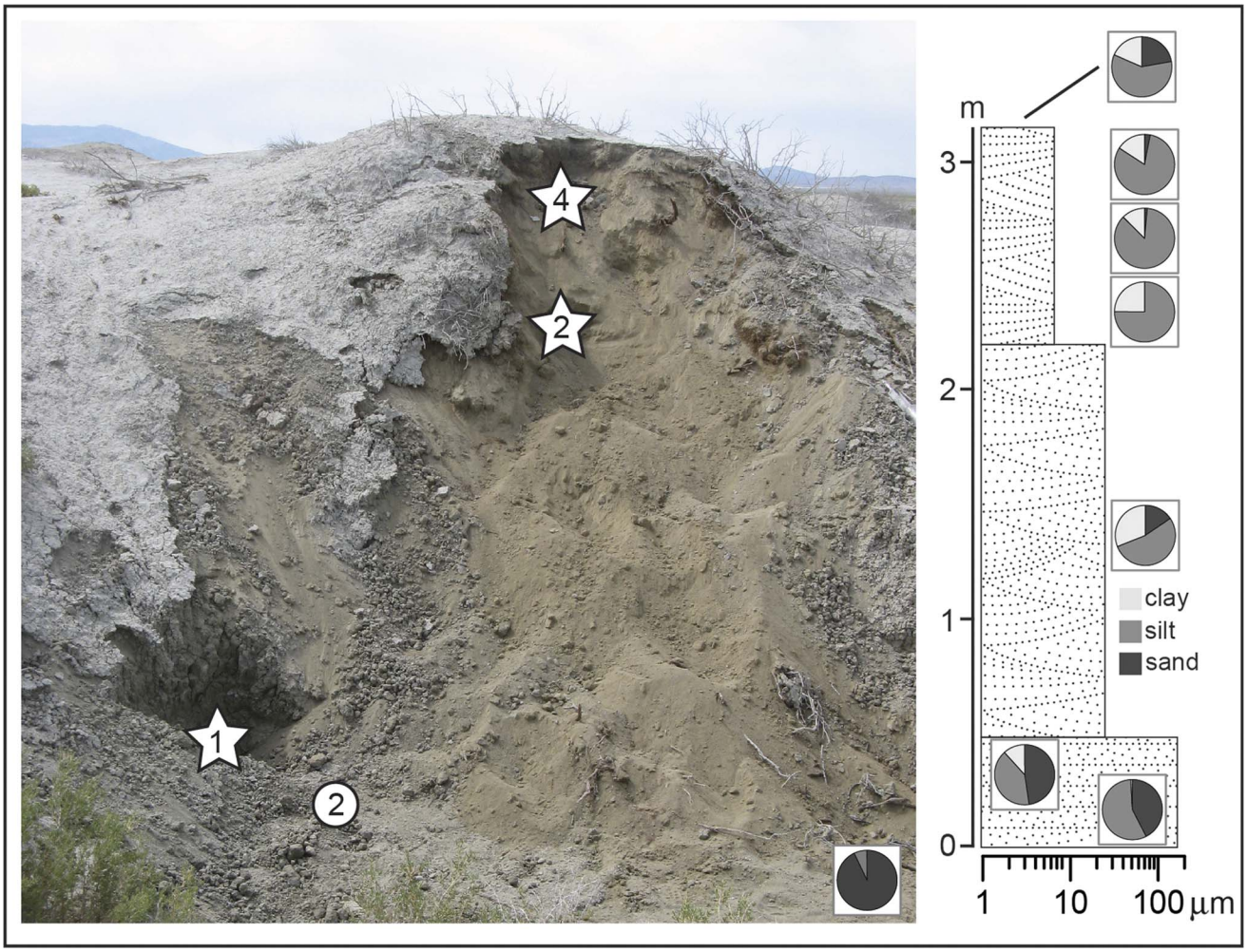

Figure 4. (color online) Field photograph, stratigraphic column, and grain-size data for the arroyo section described in 2014. The sand-dominated grain-size plot inset in the lower right corner represents the sample taken from the bed of the arroyo, out of view below the picture. Coarse sandy sediment was encountered in excavations at the base of the exposure (lower left). Luminescence age estimations were obtained on samples 14-1 (star) and 15-2 (circle) from this sandy sediment. This material was overlain by ~1.5 m of "clayey sand", which was in turn overlain by a siltier facies with upward increasing sand content. Two samples (14-2 and 14-4) collected from this facies also yielded optically stimulated luminescence ages (stars). The uppermost grain-size sample was collected from the sun-baked crust at the surface of the dune.

first and second test dose). Roughly 180 aliquots of quartz was analyzed for each sample with an acceptance rate of ~7%.

Equivalent dose was determined using the central age model (CAM) for samples with an overdispersion less than 17%, indicating focused clustering of D_e values (Galbraith et al., 1999). The internal-external consistency criterion (IEU), which has been demonstrated as a robust method for young age distributions (Thomsen et al., 2007), was applied to skewed distributions exhibiting a tail of higher D_e values. Partial bleaching by incomplete exposure to sunlight during transport is the likely mechanism responsible for skewed distributions.

Dose rates were calculated from the results of ICP-MS bulk geochemical analysis with the online Dose Rate and Age Calculator (Durcan et al., 2015) using standard conversion factors (Guérin et al., 2011), beta grain-size attenuation constants (Guérin et al., 2012), and beta etch-depth attenuation factors (Brennan, 2003). For the lone feldspar sample (14-1), an internal dose rate was calculated based on an assumed average potassium content of 10%. Direct alpha dose was assumed to be zero given that grains were etched prior to analysis. Water contents were computed after oven drying for 2 days at 65°C, with an estimated 10% uncertainty reflecting possible variation over the burial history.

Finally, a variety of additional data sources were consulted to provide context for the results from the Snow Water Lake dunes. Tree ring growth index data for *Pinus monophylla* (pinyon pine) at Pequop Summit (Site NV056), 40 km to the northeast of Snow Water Lake, were accessed from World Data for Paleoclimatology (https://www.ncdc.noaa.gov/paleo/study/4983). Climate data for Elko, Nevada, and the Clover Valley were obtained from the Western Regional Climate Center (http://www.wrcc.dri.edu/). Maps illustrating the bedrock geology of source areas for the Snow

https://doi.org/10.1017/qua.2016.5

Table 1. Samples from the Snow Water Lake dunes.

Sample	Type[a]	Latitude (DD.ddd)	Longitude (DD.ddd)	Elevation (m)	Relief[b] (m)	Depth (m)
SWOSL-14-1	OSL & GS	40 48.180°N	114 58.302°W	1706.5	0.5	2.50
SWOSL-14-2	OSL & GS	40 48.180°N	114 58.302°W	1708.0	2.0	1.50
SWOSL-14-3	OSL & GS	40 48.180°N	114 58.302°W	1708.5	2.5	1.25
SWOSL-14-4	OSL & GS	40 48.180°N	114 58.302°W	1709.0	3.0	1.00
SWOSL-15-1	OSL & GS	40 48.110°N	114 58.886°W	1707.4	1.4	1.00
SWOSL-15-2	OSL & GS	40 48.181°N	114 58.301°W	1707.0	1.0	2.50
SWOSL-15-3	OSL & GS	40 48.042°N	114 58.145°W	1716.2	10.2	0.70
SWOSL-15-4	OSL & GS	40 47.660°N	114 59.201°W	1712.3	6.3	0.70
SWOSL-15-5	OSL & GS	40 47.625°N	114 59.284°W	1711.3	5.3	0.70
SWOSL-15-6	OSL & GS	40 47.481°N	114 59.786°W	1713.6	7.6	0.70
Arroyo surface	GS	40 48.180°N	114 58.302°W	1706.5	–	–
Dune crust	GS	40 48.180°N	114 58.302°W	1709.0	–	–
Playa surface	GS	40 48.180°N	114 58.617°W	1706.0	–	–
Clayey-sand	GS	40 48.180°N	114 58.302°W	1707.0	–	–

[a]GS, grain-size analysis; OSL, optically stimulated luminescence.
[b]Above playa surface.

Water Lake playa in the East Humboldt Mountains were downloaded from the US Geological Survey National Geologic Map Database (http://ngmdb.usgs.gov/maps/mapview/).

RESULTS

Grain size

Sediment samples from the Snow Water Lake dunes are classified as silty clay loams with an average of 11% sand, 72% silt, and 16% clay (Table 2). Median grain size for dune samples ranges from 6 to 26 μm. The five samples collected directly from dune crests (15-1, 15-3, 15-4, 15-5, and 15-6) exhibit generally similar grain-size distributions with a modal grain size of medium to coarse silt (~15%–25% of the total distribution). There is some spatial variability; for instance, sample 15-4 contains three times as much sand as sample 15-5, collected just 130 m away. Similarly, the three samples within the dune excavated at the arroyo site (14-2, 14-3, and 14-4) are finer than the others, with a modal grain size of very fine to fine silt (26%–43%). Yet sample 15-3, collected from 330 m to the south–southeast in the same dune cluster, contains ~20% sand. Sample 15-1, collected from the dune island (Fig. 1), has the greatest sand content of all dune samples (28%).

Samples from elsewhere in the study area exhibit a variety of textures (Table 2). For instance, a sedimentary facies characterized in the field as "clayey sand" was encountered in many reconnaissance excavations and was sampled at the arroyo site in 2014 (Fig. 4). The sand content of this material (16%) is similar to that of the dune samples. However, the clay content is much higher, 31% compared with the average of 16% in the dune samples, yielding an overall textural class of silty-clay loam. In contrast, sand comprises only 2% of a sample obtained from the playa surface (Fig. 1); 42% of this sample is clay. The coarsest sample, with 93% sand and no detectable clay, was collected from the channel at the 2014 arroyo site (Fig. 4). A similar, although less pronounced, sand-dominated distribution was also measured for the 14-1 and 15-2 samples collected from the base of this exposure (Fig. 4).

Mineralogy

XRD analysis reveals that quartz and calcite are the most common minerals in the dune sands, with lesser amounts of plagioclase. Oriented slides of the clay fraction are dominated by a mineral with a 10Å *d*-spacing. This spacing does not collapse after heating at 100°C for 1 h, indicating that this mineral is dioctahedral clay.

The overall mineralogical composition is consistent across the samples analyzed, although the relative abundance of these minerals varies between dune clusters. In general, dunes from the southern part of the study area have much greater abundances of calcite, whereas dunes along the northern and eastern part of the playa are dominated by quartz. Calcite/quartz peak area ratios are <1 for sand-dominated samples from the arroyo site, average ~5 for samples from the northeastern dunes, and reach values in excess of 35 for dunes along the south side. Relatively high (~20) values were also calculated for samples 14-2 and 14-2 from deeper within the deposits of the dune at the arroyo site, and a very high value of 77 was measured for the clayey sand from the central part of this dune.

Geochemistry

Geochemical analysis with ICP-MS permits further comparison of the dune samples (Table 3). After Si, Ca is the most abundant of the measured major elements, averaging 10.1%. Mg and Al are similar (~4%), as are K, Na, and Fe (~2%). Ti is the least abundant of the measured major elements, averaging just 0.2%. Sr is the most abundant of the measured trace elements, averaging 1137 ppm. P, Ba, and Mn are also present at concentrations averaging >100 ppm. Zr, V, Ce, Cr, La, and

https://doi.org/10.1017/qua.2016.5

Table 2. Grain-size data for samples from the Snow Water Lake dunes.

Sample (material)	Mean (μm)	Median (μm)	Mode (μm)	Standard deviation (μm)	CV (%)	Textural class	Total sand (%)	C sand (%)	M sand (%)	F sand (%)	VF sand (%)	Total silt (%)	C silt (%)	M silt (%)	F silt (%)	VF silt (%)	Clay (%)
14-2 (Dune)	7.0	5.8	8.2	6.7	95.9	SiL	0	0.0	0.0	0.0	0.0	75	1.2	10.8	29.5	33.6	24.9
14-3 (Dune)	14.0	9.4	10.8	14.7	104.4	SiL	2	0.0	0.0	0.0	1.5	86	10.7	21.8	27.2	26.2	12.6
14-4 (Dune)	11.4	6.0	7.2	25.5	223.0	SiL	3	0.0	0.1	1.5	1.5	81	2.2	8.3	27.8	42.8	15.8
15-1 (Dune)	45.6	26.1	72.0	54.1	118.5	SiL	28	0.0	1.1	7.0	19.7	56	19.8	12.9	9.9	13.3	16.3
15-3 (Dune)	41.2	14.3	14.2	68.2	162.7	SiL	19	0.2	2.6	5.0	11.2	64	15.3	16.1	14.9	18.1	16.6
15-4 (Dune)	30.1	18.0	51.6	33.9	112.7	SiL	15	0.0	0.1	2.0	12.6	71	22.6	18.7	13.5	16.2	14.4
15-5 (Dune)	20.4	13.3	15.2	22.3	109.5	SiL	5	0.0	0.0	0.4	4.5	82	18.8	24.6	19.8	18.4	13.6
15-6 (Dune)	33.2	20.7	55.3	35.5	107.1	SL	19	0.0	0.0	2.2	16.6	64	23.4	15.3	10.6	14.5	17.3
14-1 (Basal)	172.2	29.8	18.6	210.6	122.3	SL	42	8.9	24.2	7.8	1.6	57	7.4	28.9	14.5	5.9	0.9
15-2 (Basal)	177.8	50.1	488.2	236.0	132.8	L	48	12.7	15.3	11.0	8.6	41	7.0	10.6	10.9	12.2	11.7
Arroyo surface	749.1	565.5	632.4	651.0	86.9	Sand	93	56.6	25.2	9.3	1.9	7	0.8	1.6	2.2	2.4	0.1
Dune crust	37.4	12.8	72.3	51.7	138.0	SiL	22	0.0	0.8	6.3	15.2	59	14.5	11.7	12.4	20.7	18.5
Playa surface	8.4	2.8	3.2	15.8	187.4	SiC	2	0.0	0.0	0.1	2.2	56	5.8	6.9	11.1	32.3	41.6
Clayey sand	27.1	5.4	4.2	45.9	169.2	SiCL	16	0.0	0.5	4.3	10.8	53	11.3	8.3	9.9	23.9	31.1

Note: C.V., Coefficient of Variation; SiL, Silt Loam; L, Loam; SL, Sandy Loam; SiC, Silty Clay; SiCL, Silty Clay Loam; C, Coarse; M, Medium; F, Fine; VF, Very Fine.

Table 3. Summary statistics for geochemical analysis of dune samples.

Statistic	Al (%)	Ba (ppm)	Ca (%)	Ce (ppm)	Cr (ppm)	Cs (ppm)	Fe (%)	Ga (ppm)	Hf (ppm)	K (%)	La (ppm)	Mg (%)	Mn (ppm)	Na (%)	Nb (ppm)	P (ppm)	Rb (ppm)	Si (%)	Sn (ppm)	Sr (ppm)	Ta (ppm)	Th (ppm)	Ti (%)	U (ppm)	V (ppm)	W (ppm)	Y (ppm)	Zr (ppm)
Mean	3.8	581.9	10.1	32.0	23.9	11.2	1.7	9.7	2.3	2.3	17.4	4.7	366.3	1.9	6.8	867.5	92.7	45.1	1.1	1137.6	0.5	6.5	0.2	2.4	49.6	1.7	10.0	84.4
Median	3.7	525.0	11.4	31.0	21.5	11.8	1.8	9.5	2.2	2.4	16.6	5.3	379.0	1.9	7.0	850.0	90.1	37.4	1.0	1182.5	0.5	6.3	0.2	2.2	53.5	1.9	9.9	80.5
Standard deviation	0.26	133.44	2.39	4.38	5.19	3.16	0.25	0.68	0.90	0.10	2.59	1.24	79.65	0.38	0.86	337.04	5.91	12.80	0.16	274.46	0.07	0.83	0.01	0.68	11.29	0.45	0.49	34.40
Skewness	0.61	0.90	–0.96	1.18	0.46	–0.79	–1.11	0.53	0.35	–0.48	1.72	–1.03	–0.32	0.00	0.44	0.08	0.64	1.11	1.03	–0.60	–0.28	1.66	–0.79	0.62	–1.21	–0.81	0.19	0.51
Minimum	3.5	443.0	5.8	26.6	18.0	5.3	1.2	9.0	1.1	2.2	14.8	2.4	232.2	1.3	5.5	460.0	84.9	35.1	1.0	656.0	0.4	5.7	0.1	1.7	27.0	1.0	9.2	42.2
Maximum	4.2	822.0	12.1	40.7	30.0	15.2	1.9	10.7	3.6	2.4	23.0	6.0	464.4	2.4	8.4	1300.0	102.5	64.6	1.4	1520.0	0.6	8.3	0.2	3.5	62.0	2.0	10.8	135.0

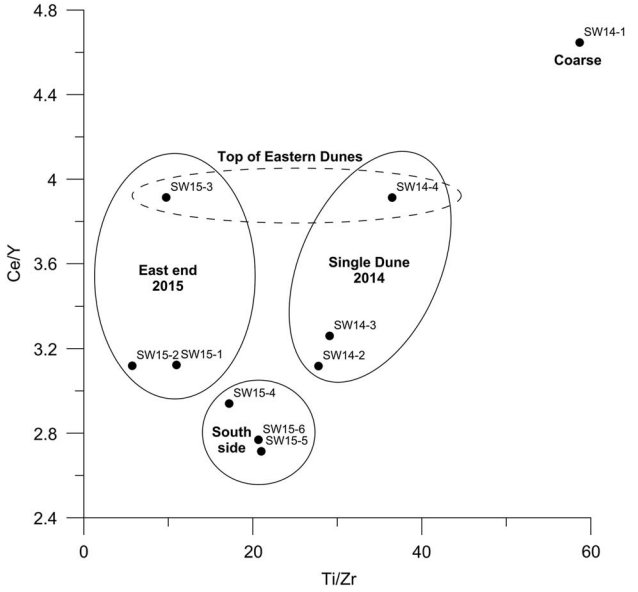

Figure 5. Scatter plot showing elemental ratios Ti/Zr versus Ce/Y. Dunes along the south side of the playa cluster in a different field than those at the east end. The coarse sediment from the base of the 2014 exposure (14-1) is an obvious outlier.

Cs are present at average concentrations between 10 and 100 ppm. Ga, Nb, Th, U, Hf, W, Sn, and Ta are present at concentrations <10 ppm. Values of Ca and Sr are strongly positively correlated ($r^2 = 0.8629$). Ca and Ba are also strongly correlated ($r^2 = 0.9452$) but in a negative direction.

Scatter plots of the elemental ratios Ce/Y and Ti/Zr reveal spatial clustering of samples (Fig. 5). The three samples collected along the south side of the playa (15-4, 15-5, and 15-6) plot in a cluster distinct from the dunes sampled at the northeast end of the playa. The three samples from within the dune at the arroyo in 2014 also appear in a distinct field. The two samples from the crest of the easternmost dune cluster (14-4 and 15-3) have much higher Ce/Y and plot apart from the other dune samples. This grouping by elemental abundance mirrors the pattern exhibited by the mineralogical composition of the dune samples, suggesting that the sediment comprising the dunes adjacent to different parts of the Snow Water Lake playa may be sourced from different regions.

Luminescence ages

Luminescence ages were determined for seven samples: five from dunes and two from the coarser sediment at the base of the 2014 exposure. One sample (14-1) was analyzed for both optically stimulated luminescence (OSL) on quartz and infrared-stimulated luminescence (IRSL) on feldspar; thus a total of eight luminescence ages were calculated (Table 4). The number of aliquots passing quality-control inspections averaged 18 for each sample.

The results split into two age clusters (Table 4) with the older cluster composed entirely of ages from dunes. Sample 15-1, from the dune "island" in the playa (Fig. 1), has the oldest apparent age (AD 1696 ± 81). Samples 14-2 and 14-4,

Table 4. Luminescence ages for the Snow Water Lake dunes.

Sample name	Lab number	D_e (Gy)	1 SE (Gy)	Dose rate (Gy/ka)	1σ (Gy/ka)	n (aliquots)	Skew	Kurtosis	OD (%)	U (ppm)	Th (ppm)	K (wt. %)	Rb (ppm)	H_2O (%)	CAM (ka)	1σ (ka)	IEU (ka)	1σ (ka)	Preferred model	Age (yr AD)	1 SE (yr)
SW14-1	M30	0.60	0.19	3.30	0.09	22	3.0	12.6	2.4	1.2	6.6	2.5	92.4	3.5	0.18	0.06	–	–	CAM	1835	57
SW14-1	M30k	0.71	0.06	3.70	0.09	18	0.8	3.1	1.6	1.2	6.6	2.5	92.4	3.5	0.20	0.02	–	–	CAM	1816	18
SW14-2	M31	0.92	0.46	3.20	0.09	11	0.3	1.6	0.0	3.2	6.3	2.4	102.5	16.0	0.29	0.14	–	–	CAM	1729	143
SW14-4	M33	1.08	0.25	3.50	0.09	16	2.1	6.4	23.1	3.5	6.3	2.4	99.2	19.1	0.54	0.20	0.31	0.07	IEU	1706	72
SW15-1	M80	2.26	0.34	3.21	0.09	25	2.9	11.2	19.0	1.9	6.5	2.4	89.7	8.8	0.36	0.05	0.32	0.08	IEU	1696	81
SW15-2	M81	0.02	0.07	2.89	0.11	24	2.4	9.8	26.2	1.3	4.7	2.3	78.7	4.9	0.01	0.02	–0.04	0.02	CAM	2009	25
SW15-3	M82	0.82	0.21	3.48	0.12	16	1.9	6.8	17.1	1.7	8.3	2.4	84.9	15.5	0.32	0.09	0.24	0.06	IEU	1780	62
SW15-4	M83	0.72	0.61	2.90	0.10	5	0.3	1.3	0.0	2.2	5.7	2.2	89.1	11.6	0.25	0.21	–	–	CAM	1768	211

Note: CAM, central age model; D_e, equivalent dose; IEU internal-external consistency criterion; SE, Standard Error; OD, Overdispersion.

https://doi.org/10.1017/qua.2016.5

collected from within the top ~1 m of the dune at the arroyo site (Fig. 4), yield ages of AD 1729 ± 143 and AD 1706 ± 72, respectively. Sample 15-3 from stratified sediment at the top of the eastern dune cluster (Fig. 2D) yielded the youngest age of AD 1780 ± 62. Sample 15-4, the only dated sample from the south side of the playa (Fig. 1), returned a relatively imprecise age of AD 1768 ± 211 because of limited quartz. Even given the uncertainty typical of the luminescence technique on very young deposits, it is notable that all of these ages overlap between AD 1725 and 1775, centering strongly on AD 1750. In contrast, OSL and IRSL analysis of a sample from the coarser sediment exposed at the base of the 2014 arroyo exposure (14-1) yielded younger ages of AD 1835 ± 57 and AD 1816 ± 18, respectively (Fig. 4). The apparent difference in age between the dunes and the arroyo sediment is not a function of the age model used; calculating ages for dune samples 14-4, 15-1, and 15-3 using the CAM, which is not supported by their relatively large skewness and kurtosis values (Table 4), yields age estimates that are even older, widening the apparent temporal gap between the two age clusters. Thus, it appears that the dunes were last accumulating during the mid-eighteenth century, whereas the sediment in the arroyo was deposited sometime later.

The result for sample 15-2, from the base of the arroyo section, is enigmatic (Table 4). The D_e distribution for this sample has a large overdispersion value (26.2%) indicating that the IEU model is more appropriate. However, this model returned a negative age, and the CAM yields an age of AD 2009 ± 25. Given the consistent set of field and laboratory protocols followed in sample collection and processing, it is unlikely this sample was inadvertently bleached. In the field, this sediment exhibited clear stratigraphy but must have been a modern deposit layered onto the arroyo wall, not a coarse basal unit underlying the dune.

DISCUSSION

Dune morphology and composition

As is clear from Figure 1, the dunes adjacent to the Snow Water Lake playa are concentrated in discrete clusters. Four of these are located along the north side of the playa, two are on the south, one large cluster is at the eastern end of the study area, and one rises as an island from the playa surface. The position of these clusters is consistent with the westerly and southwesterly prevailing wind directions recorded at Elko, Nevada, from March through October, and with the resultant drift direction of east–northeast calculated from the Elko record (Jewell and Nicoll, 2011). No dunes are present to the west of the playa, suggesting that easterly winds are less effective at mobilizing sediment from the playa surface. This may be because the generally lower mean wind speeds during winter when easterly winds are most common (15% of the time), or because playa sediment is more likely to be frozen at that time.

The sedimentology of these dunes differs from the classic "sand dune" dominated by coarse material. Samples collected for grain-size analysis do contain sand (Fig. 1, Table 2), but at generally low abundances (max of 28%) and with clay contents in excess of 15%. In this regard, the Snow Water Lake dunes resemble a hybrid between classic "sand dunes" and features known as "clay dunes" described from a diverse array of settings (e.g., Coffey, 1909; Huffman and Price, 1949; Price, 1963; Bowler, 1973; Holliday, 1997). Clay dunes are associated with neighboring shallow depressions that seasonally flood and desiccate. Drying of the fine-grained sediment lining the floor of a depression leads to desiccation cracking and curling that makes the sediment surface vulnerable to eolian deflation. Mechanical disintegration of these surface fragments through saltation produces sand-sized aggregates of finer sediment. Fine-textured particles can also adhere to salt crystals forming larger composites (Young and Evans, 1986). Aggregates formed by either process are transported downwind, along with sand grains sensu stricto where they accumulate around clumps of vegetation at the margin of the depression, eventually coalescing to form dunes (Coffey, 1909). This mode of formation appears viable for the Snow Water Lake dunes given their position relative to the playa, the grain-size distribution of the dune sediments, and the wind data available for Elko, Nevada. Furthermore, reworking of sediment from older dunes is common in small dunes adjacent to depressions and often leads to considerable heterogeneity in sediment properties and luminescence ages within individual dune forms (Telfer and Thomas, 2006). Such reworking, along with heterogeneity in the sand content of sediment at the surface of the playa, could explain the contrasting sand abundances noted over short spatial scales in the dune crest samples at Snow Water Lake.

In comparison with other dunes reported in the literature (Muhs, 2004), the sediment comprising the Snow Water Lake dunes is mineralogically immature. Measured abundances of SiO_2 range from ~35% to 65%, whereas the sum of K_2O, Na_2O, and Al_2O_3 has a tighter range from 11.7% to 12.9%. In contrast, dunes considered mineralogically mature typically have SiO_2 contents in excess of 90% and very low feldspar abundances (Muhs, 2004). Weathering and eolian processes generally eliminate feldspars over time, concentrating quartz. Thus, mineralogically immature dunes are either young or have inherited a distinctly quartz-poor composition from their source material (or both). Small spatial scales and short transport distances may also play a role in retaining feldspars and reducing quartz dominance. Together, the mineralogical immaturity of the dune sediments and the partial bleaching noted in the luminescence results for some of these samples suggest that the distance of eolian transport from source to sink was short. This insight further supports the interpretation of the Snow Water Lake dunes as hybrid sand and clay dunes formed by eolian deflation of fine sediment from the adjacent playa.

Dune ages

The five luminescence ages determined for samples retrieved from excavations into the tops of dunes overlap between AD 1725 and 1775 (Table 4). This convergence is a strong indication that these dunes were accumulating in the mid-eighteenth century. Episodes of dune accumulation at this time have been reported from elsewhere in the Great

https://doi.org/10.1017/qua.2016.5

Basin and southwestern United States. For instance, a study of Holocene dunes in the Ash Meadows National Wildlife Refuge of southern Nevada reported an OSL age of 200 ± 20 yr BP (Lancaster and Mahan, 2012). Similarly, IRSL dating of feldspars from dunes in the Mojave Desert yielded ages of 250 ± 70, 215 ± 40, 200 ± 25, and 155 ± 50 yr BP (Clarke et al., 1995), matching previously reported results (Edwards, 1993). In a synthesis of available data, Halfen et al. (2016) noted the latest Holocene dune accumulation ca. 0.4, 0.25, and 0.11 ka BP, and two episodes of sand accumulation in the past millennium were reported at the Skull Creek dunes in southeastern Oregon (Mehringer and Wigand, 1986). Collectively, these results evidence an episode of generally synchronous dune accumulation in this region during the interval following the Medieval Climate Anomaly (~AD 900–1300) and preceding the classical ~AD 1850 peak of the Little Ice Age (Stine, 1994; Grove, 2004).

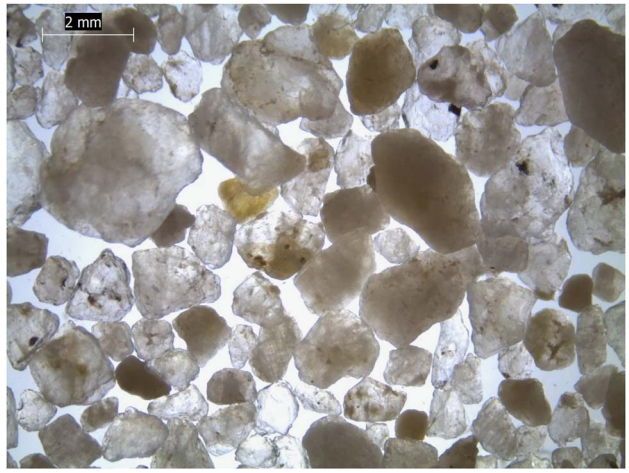

Figure 6. (color online) Photograph of quartz (clear) and feldspar (translucent) sand grains from sample 15-3 under magnification and transmitted light. The angular nature of most grains is obvious, as is the lack of surface frosting typical of grains that have experienced long-distance eolian transport.

Paleoclimate implications

It is intuitive to associate intervals of dune accumulation with heightened aridity, and that connection is likely valid in many geomorphic settings, for instance the High Plains of the central United States (e.g., Forman et al., 1992, 1995; Muhs and Maat, 1993; Muhs and Holliday, 1995). In the Great Basin and southwestern United States, however, studies have proposed an alternative theory that dune accumulation is limited by sediment supply and that intense precipitation events are required to deliver sediment to playa surfaces (e.g., Clarke and Rendell, 1998; Lancaster and Mahan, 2012; Lancaster et al., 2015; Halfen et al., 2016). Related studies have suggested that the seasonality of precipitation may be more important than the overall amount (Miller et al., 2010). Connections have been demonstrated between alluvial fan activity and intensity of the El Niño–Southern Oscillation climatic pattern (Bacon et al., 2010).

The model connecting dune activity to sediment supply provides a context in which to evaluate the dunes at Snow Water Lake. As discussed previously, the Snow Water Lake dunes resemble clay dunes with a varying sand component. Under magnification, many of these sand grains are strikingly coarse and angular, resembling fresh grus eroded from the metamorphic rocks in the East Humboldt Mountains to the west (Fig. 6); they are very distinct from the rounded and frosted grains typical of far-traveled eolian sediment. However, coarse grus cannot make it across the alluvial fans to the playa (~10 km; Fig. 1B) without high-volume stream flow from the mountains. High-volume flows also deliver fines that resurface sections of the playa inundated by floodwaters (Fig. 3), as was observed during historic flooding events on the Mojave River (Clarke and Rendell, 1998). Thus dune growth appears connected to wet conditions that transport sediment to the playa, as reported by previous studies (Clarke and Rendell, 1998; Lancaster and Mahan, 2012).

Further support for this interpretation is provided by the pattern of mineralogical and geochemical differences between the dune clusters. The dunes along the south side of the playa, which have much greater calcite/quartz ratios and Ca contents along with distinct trace element signatures (Fig. 5), are located just to the east of the point where Warm Creek debouches onto the playa when flowing (Fig. 1B). Geologic maps indicate that the headwaters of Warm Creek are predominantly underlain by carbonates of the Pennsylvanian-age Park City and Pequop Formations (Hope and Coats, 1976). In contrast, the dune clusters studied to the north and east, which are dominated by quartz, are located near where Wiseman Creek reaches the playa. Wiseman Creek drains an area of the East Humboldt Mountains underlain by a Lower Paleozoic and Precambrian metamorphic core complex containing granitic to dioritic gneisses, mica schists, and quartzites (Hope and Coats, 1976). This pattern strongly suggests that these dune clusters grow through accumulation of sediment derived primarily from the immediately adjacent playa surface, and that the properties of sediment on the playa surface are most closely linked to the nearest entering stream. Thus, a wetter climate with more frequent flooding events sets the stage for dune growth.

Recent and prehistoric climate data for the Snow Water Lake area are available from several sources. Tree ring data from Pequop Summit, ~40 km northeast of the Snow Water Lake dunes, extend from AD 1980 back to AD 1500. A long precipitation record from Elko, Nevada, begins in AD 1888, although some months are missing from years in the first few decades. For the period of overlap between the tree ring data and the most complete part of the Elko precipitation record (AD 1917–1980), the tree ring growth index is correlated with precipitation on a water year basis (October–September). The coefficient of determination for this relationship is low on an annual basis (0.261) and is somewhat higher (0.353) when data are smoothed with a 3 yr average. Nonetheless, the striking visual correspondence strongly suggests that the tree rings are tracking precipitation (Fig. 7A).

https://doi.org/10.1017/qua.2016.5

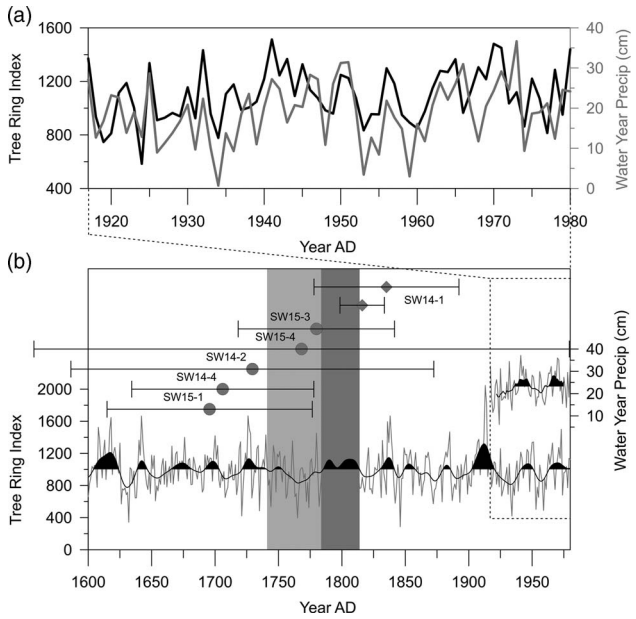

Figure 7. Luminescence ages compared with local tree ring records and precipitation data. (A) Tree ring growth indices from Pequop Summit (Site NV056), 40 km northeast of Snow Water Lake at an elevation of 2286 m (black line), exhibit strong correlation with measured precipitation data at Elko, Nevada, ~70 km to the west (gray line). (B) The five dune optically stimulated luminescence (OSL) ages (circles) overlap strongly with a prolonged interval of low growth index in the latter 1700s (light gray band), implying drought conditions. This interval was preceded by a decade of very high growth index values, including the highest in a 150-yr stretch, suggesting very wet conditions. Another wet period centered on AD 1800 (dark gray band) aligns with the paired OSL and infrared-stimulated luminescence ages for the sand diamonds at the base of the 2014 exposure (14-1), suggesting that a return to wet conditions led to arroyo cutting and deposition of the sand as a channel lag banked against the base of the dunes.

Given this correspondence, it is notable that the five OSL ages from the Snow Water Lake dunes align with a prolonged mid-eighteenth-century drought (below average growth index) that followed a relatively wet interval (high growth index) in the 1720s (Fig. 7B). Years AD 1726–1728 had particularly vigorous tree growth, with 1726 achieving the highest value in ~150 yr (1642–1789). If the tree rings are tracking precipitation, then this relationship suggests that the extremely wet years of the 1720s brought large amounts of sediment to the Snow Water Lake playa, which was then redistributed into dunes during a multidecadal drought in the latter half of the 1700s. This interpretation does not require that the dunes were constructed entirely in the 1700s, only that an episode of dune accumulation occurred then. Geographic Information System analysis indicates that the total dune volume corresponds to a layer of sediment ~50 cm thick across the playa surface, an amount that seems an unreasonable to have been deposited and eroded in a single switch from wet to dry conditions. Instead, it is logical that other decadal-scale switches from wet to dry conditions drove pulses of dune growth. Such events would not be captured by our sampling strategy, which focused on sediment collected from near the current dune crests. No evidence was found for dune accumulation in response to the switch from wet conditions in the 1920s to drought in the 1930s. Such evidence may have been lost to more recent erosion given the amount of surface lowering of the dunes revealed by the perched shrubs and root pedestals.

The mid-1700s drought seen in the tree ring record was followed by a stretch of above-average tree growth centered on AD 1800 (Fig. 7). This timing matches the OSL and IRSL ages for SW14-1 at the 2014 arroyo site (Fig. 7), suggesting that a shift to increased precipitation eroded the arroyo and deposited this coarse sand banked against the base of the dunes.

The southwestern United States is currently is the midst of a prolonged drought that began in 2001 (MacDonald, 2010). Given this model of sediment delivery to the Snow Water Lake playa, decreased precipitation is one potential explanation for why the dunes are currently eroding. Diversions of surface water for irrigation and livestock also increased steadily following settlement of the Clover Valley in the late 1800s. Based on analysis of data from the Nevada Water Rights Databases (http://water.nv.gov/waterrights/), permitted diversions now total ~10 m^3/s, with an annual duty in excess of 20,000 ac. ft. The combined impact of climatic drought and artificial water diversions, therefore, is likely playing a causal role in the current eroding of the dunes.

An important limitation of this study is the reliance on dune crest ages as opposed to deep stratigraphic sections. This shortcoming, imposed by realities of the fieldwork and project scope, precludes interpretation of the history of these dunes prior to deposition of the sediment currently forming the dune crests in the eighteenth century. Future work should focus further on the three-dimensional distribution of sediment types and ages within the dunes. This could involve expanded field reconnaissance to identify additional natural exposures, excavation of larger artificial exposures, subsurface sampling through auguring, and geophysical analysis with ground penetrating radar (e.g., Lindhorst and Betzler, 2016). Similar dunes associated with playas in pluvial lake basins, such as those in the Ruby Valley ~50 km to the southwest, could also be studied to develop a more complete chronology for dune activity in this region. This advance would be an important step toward better elucidating paleoclimate information from eolian deposits in this part of the Great Basin (Halfen et al., 2016).

CONCLUSIONS

Clusters of dunes adjacent to the Snow Water Lake playa in Elko County, Nevada, are constructed from sediment eroded from the playa surface by prevailing southwest to northwest winds. The dunes contain coarse, angular sand grains intermixed with finer silt and clay and are mineralogically immature. All dunes contain calcite, quartz, and dioctahedral clay, with minor amounts of plagioclase; however, calcite dominates dunes along the south side of the playa, whereas

https://doi.org/10.1017/qua.2016.5

quartz is more abundant in dunes to the north and east. This pattern matches the lithologies underlying the headwaters of streams that reach the playa near the dune clusters. Luminescence (OSL and IRSL) dating demonstrates that the dunes were accumulating in the mid-eighteenth century. Moisture-sensitive tree ring records document a multidecadal drought at that time, which followed an extremely wet decade in the 1720s. Years with above-average precipitation, therefore, may have delivered sediment to the playa that was then reworked into the dunes during the subsequent drought. Younger luminescence ages from a sand-dominated unit exposed in an arroyo cut through the dunes may reflect a wetter, more erosive climatic regime ~AD 1800. The dunes are currently eroding because the amount of sediment reaching them has been reduced, perhaps because of climatic shifts and postsettlement diversions of surface water. Continued erosion could result in the loss of these features.

ACKNOWLEDGMENTS

This work was supported by Middlebury College. Thanks to Pete Ryan and Scott Munroe for their help with the XRD analysis. Thoughtful comments by Nick Lancaster, Jim O'Connor, and two anonymous reviewers greatly improved the manuscript.

REFERENCES

Ahlbrandt, T.S., Fryberger, S.G., 1980. Eolian deposits in the Nebraska Sand Hills. *US Geological Survey Professional Paper* 1120, 1–24.

Bacon, S.N., McDonald, E.V., Caldwell, T.G., Dalldorf, G.K., 2010. Timing and distribution of alluvial fan sedimentation in response to strengthening of late Holocene ENSO variability in the Sonoran Desert, southwestern Arizona, USA. *Quaternary Research* 73, 425–438.

Bowler, J.M., 1973. Clay dunes: their occurrence, formation and environmental significance. *Earth-Science Reviews* 9, 315–338.

Brennan, B., 2003. Beta doses to spherical grains. *Radiation Measurements* 37, 299–303.

Bureau of Land Management, 2012. Snow Water Lake and Warm Creek allotments grazing permit renewal: Standards and guidelines for rangeland health assessment. *File 4130*, 75 pp.

Buylaert, J., Murray, A.S., Thomsen, K.J., Jain, M., 2009. Testing the potential of an elevated temperature IRSL signal from K-feldspar. *Radiation Measurements* 44, 560–565.

Clarke, M.L., Rendell, H.M., 1998. Climate change impacts on sand supply and the formation of desert sand dunes in the southwest USA. *Journal of Arid Environments* 39, 517–531.

Clarke, M.L., Richardson, C., Rendell, H., 1995. Luminescence dating of Mojave Desert sands. *Quaternary Science Reviews* 14, 783–789.

Coffey, G.N., 1909. Clay dunes. *Journal of Geology* 17, 754–755.

Durcan, J.A., King, G.E., Duller, G.A., 2015. DRAC: dose rate and age calculator for trapped charge dating. *Quaternary Geochronology* 28, 54–61.

Edwards, S.R., 1993. Luminescence dating of sand from the Kelso Dunes, California. *Geological Society, London, Special Publications* 72, 59–68.

Forman, S.L., Goetz, A.F., Yuhas, R.H., 1992. Large-scale stabilized dunes on the High Plains of Colorado: understanding the landscape response to Holocene climates with the aid of images from space. *Geology* 20, 145–148.

Forman, S.L., Oglesby, R., Markgraf, V., Stafford, T., 1995. Paleoclimatic significance of late Quaternary eolian deposition on the Piedmont and High Plains, central United States. *Global and Planetary Change* 11, 35–55.

Galbraith, R.F., Roberts, R.G., Laslett, G.M., Yoshida, H., Olley, J.M., 1999. Optical dating of single and multiple grains of quartz from Jinmium rock shelter, northern Australia: Part I, experimental design and statistical models. *Archaeometry* 41, 339–364.

Grayson, D.K., 2011. *The Great Basin: A Natural Prehistory*. University of California Press, Berkeley.

Grove, J.M., 2004. *Little Ice Ages: Ancient and Modern*. Routledge, London.

Guérin, G., Mercier, N., Adamiec, G., 2011. Dose-rate conversion factors: update. *Ancient TL* 29, 5–8.

Guérin, G., Mercier, N., Nathan, R., Adamiec, G., Lefrais, Y., 2012. On the use of the infinite matrix assumption and associated concepts: a critical review. *Radiation Measurements* 47, 778–785.

Halfen, A.F., Lancaster, N., Wolfe, S., 2016. Interpretations and common challenges of aeolian records from North American dune fields. *Quaternary International* 410, 75–95.

Holliday, V.T., 1997. Origin and evolution of lunettes on the High Plains of Texas and New Mexico. *Quaternary Research* 47, 54–69.

Hope, R.A., Coats, R.R., 1976. Preliminary Geologic Map of Elko County, Nevada. 1:100,000. US Geological Survey, Reston, VA.

Huffman, G.G., Price, W.A., 1949. Clay dune formation near Corpus Christi, Texas. *Journal of Sedimentary Research* 19, 118–127.

Jewell, P.W., Nicoll, K., 2011. Wind regimes and aeolian transport in the Great Basin, USA. *Geomorphology* 129, 1–13.

Kreutzer, S., Schmidt, C., Fuchs, M.C., Dietze, M., Fischer, M., Fuchs, M., 2012. Introducing an R package for luminescence dating analysis. *Ancient TL* 30, 1–8.

Lancaster, N., Baker, S., Bacon, S., McCarley-Holder, G., 2015. Owens Lake dune fields: composition, sources of sand, and transport pathways. *Catena* 134, 41–49.

Lancaster, N., Mahan, S.A., 2012. Holocene dune formation at Ash Meadows National Wildlife Area, Nevada, USA. *Quaternary Research* 78, 266–274.

Lindhorst, S., Betzler, C., 2016. The climate-archive dune: sedimentary record of annual wind intensity. *Geology* 44, 711–714.

MacDonald, G.M., 2010. Climate change and water in southwestern North America special feature: water, climate change, and sustainability in the southwest. *Proceedings of the National Academy of Sciences of the United States of America* 107, 21256–21262.

Mehringer, P.J., Wigand, P.E., 1986. Holocene history of Skull Creek Dunes, Catlow Valley, southeastern Oregon, USA. *Journal of Arid Environments* 11, 117–138.

Miller, D.M., Schmidt, K.M., Mahan, S.A., McGeehin, J.P., Owen, L.A., Barron, J.A., Lehmkuhl, F., Löhrer, R., 2010. Holocene landscape response to seasonality of storms in the Mojave Desert. *Quaternary International* 215, 45–61.

Muhs, D.R., 2004. Mineralogical maturity in dunefields of North America, Africa and Australia. *Geomorphology* 59, 247–269.

Muhs, D.R., Holliday, V.T., 1995. Evidence of active dune sand on the Great Plains in the 19th century from accounts of early explorers. *Quaternary Research* 43, 198–208.

https://doi.org/10.1017/qua.2016.5

Muhs, D.R., Holliday, V.T., 2001. Origin of late Quaternary dune fields on the Southern High Plains of Texas and New Mexico. *Geological Society of America Bulletin* 113, 75–87.

Muhs, D.R., Maat, P., 1993. The potential response of eolian sands to greenhouse warming and precipitation reduction on the Great Plains of the U.S.A. *Journal of Arid Environments* 25, 351–361.

Muhs, D.R., Stafford, T.W., Cowherd, S.D., Mahan, S.A., Kihl, R., Maat, P.B., Bush, C.A., Nehring, J., 1996. Origin of the late Quaternary dune fields of northeastern Colorado. *Geomorphology* 17, 129–149.

Muhs, D.R., Wolfe, S.A., 1999. Sand dunes of the northern Great Plains of Canada and the United States. *Geological Survey of Canada Bulletin* 534, 183–197.

Munroe, J.S., Laabs, B.J., 2013. Temporal correspondence between pluvial lake highstands in the southwestern US and Heinrich Event 1. *Journal of Quaternary Science* 28, 49–58.

Murray, A.S., Wintle, A.G., 2000. Luminescence dating of quartz using an improved single-aliquot regenerative-dose protocol. *Radiation Measurements* 32, 57–73.

Nevada Archaeological Association, 2000: In-Situ newsletter, 16 pp.

Price, W.A., 1963. Physicochemical and environmental factors in clay dune genesis. *Journal of Sedimentary Research* 33, 766–778.

Stine, S., 1994. Extreme and persistent drought in California and Patagonia during mediaeval time. *Nature* 369, 546–549.

Telfer, M., Thomas, D., 2006. Complex Holocene lunette dune development, South Africa: implications for paleoclimate and models of pan development in arid regions. *Geology* 34, 853–856.

Thomsen, K.J., Murray, A., Bøtter-Jensen, L., Kinahan, J., 2007. Determination of burial dose in incompletely bleached fluvial samples using single grains of quartz. *Radiation Measurements* 42, 370–379.

Young, J.A., Evans, R.A., 1986. Erosion and deposition of fine sediments from playas. *Journal of Arid Environments* 10, 103–115.

https://doi.org/10.1017/qua.2016.5